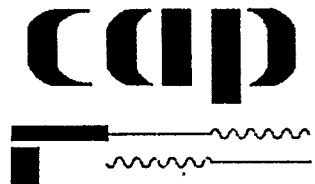

BNL#-61983
CAP 127-Muon-95R

Analysis of Pion Production Data from E-802 at 14.6 GeV/c Using ARC

David Kahana
Physics Dept., BNL, Upton, NY

and

Yağmur Torun
Physics Dept., SUNY at Stony Brook and Physics Dept., BNL

JULY 1995

CENTER FOR ACCELERATOR PHYSICS

BROOKHAVEN NATIONAL LABORATORY
ASSOCIATED UNIVERSITIES, INC.
Under Contract No. DE-AC02-76CH00016 with the
UNITED STATES DEPARTMENT OF ENERGY

BNL-61983
INFORMAL

ANALYSIS OF PION PRODUCTION DATA FROM E-802 AT 14.6 GeV/c USING ARC

David Kahana

Department of Physics

Brookhaven National Laboratory

Upton, NY 11973

Yağmur Torun

Physics Department

State University of New York

Stony Brook, NY 11794

We compared the invariant cross sections for pion production by a 14.6 GeV/c proton beam on Be, Al, Cu and Au targets from the measurements of Abbott *et. al.* with predictions of the ARC program. The agreement was found to be good in the region where data exists. Most pions are found at low momenta in the lab frame. Unfortunately very little data exists for low momentum pions.

INTRODUCTION

The pion production spectrum plays a very important role in the design of a muon collider. In the present design studies, the front end of the collider consists of a target bombarded by a proton beam. The resulting pions are collected into a decay channel for muon production. Final luminosity of the collider is proportional to the square of the number of pions collected per incident proton. The shape of the pion spectrum is an important consideration in the design of the decay channel and the initial stage of the muon beam line.

Data on inclusive pion production cross sections at low momenta is very limited in the literature. A careful analysis of the existing data is necessary to single out a working model for use in the collider design. Several models have been considered. The Wang formula [1] that has been used in earlier Monte Carlo simulations [2] is probably most appropriate for forward pion production in $p - p$ collisions at high energies [3], but it fails at low energies and large angles [4]. The Hagedorn-Ranft model [5] also doesn't seem to be well suited for reproducing the low energy part of the spectrum.

In modelling production of pions from a large nucleus it is essential to handle correctly the effect of secondary collisions, since rescattering has significant effects on the pion spectrum. One method for doing this, using known data on two body collisions, is the intranuclear cascade model. In this report, we have used the cascade code ARC (A Relativistic Cascade) to simulate pion production from Be, Al, Cu and Au targets bombarded by a 14.6 GeV/c proton beam. ARC has been extensively tested in modelling particle production in nucleus-nucleus collisions at AGS energies and has indeed predicted results for Au+Au [6]. Here we compare ARC cross sections for pion production in $p + A$ collisions with those found in the E-802 measurements.

DATA

The data from the E-802 Collaboration at the AGS [7] was retrieved from the National Nuclear Data Center database at BNL as tables of the invariant cross section I vs. transverse kinetic energy $T_\perp$, for different rapidity bins y in the lab frame. These kinematical variables are defined as:

$$I = \frac{1}{2\pi m_\perp} \frac{d^2\sigma}{dm_\perp dy}$$

$$m_\perp = \sqrt{p_\perp^2 + m_\pi^2}$$

$$T_\perp = m_\perp - m_\pi$$

$$y = \sinh^{-1}\left(\frac{p_\parallel}{m_\perp}\right) = \frac{1}{2}\ln\left[\frac{E + p_\parallel}{E - p_\parallel}\right]$$

where m_π is the pion mass, $p_{||}$ and $p_\perp$ are the longitudinal and transverse components of the pion momentum, and $c = 1$ throughout.

E-802 consists of a forward spectrometer with good particle identification up to 5 GeV/c for pions, best below 1.4 GeV/c [8]. The measurements were triggered on minimum-bias events by particles entering the spectrometer. A minimum interaction trigger was simulated in theory by counting only events in which the incoming proton interacted at least once with a nucleon. There is some sensitivity to the trigger in both theory and experiment.

The low $m_\perp$ end of the spectrum is limited by the angular acceptance of the spectrometer with a rapidity dependent cutoff. The high $m_\perp$ end is limited by statistics at low rapidities and particle identification at high rapidities. The data includes corrections for pion decay in addition to detector efficiencies. Typical errors on overall normalization of cross sections is estimated to be 10-15%. The error bars shown in the plots are statistical uncertainties only.

THEORY: ARC

ARC is a purely hadronic cascade code designed to describe heavy ion collisions at AGS energies. The model has been extensively described [9] in the literature: for the sake of clarity and convenience we summarize the main features here. The basic assumptions are:

- On-shell hadrons and low mass hadron resonances scatter incoherently. No phase information is kept. Thus, one deals with probabilities rather than amplitudes in constructing the cascade. Propagation between scatterings is purely classical.
- Relativistic kinematics are used in propagating particles, in the time ordering of hadronic collisions, and in generating final states for elementary two-body collisions.
- Only soft QCD production is modelled, essentially, the production and absorption of low $p_\perp$ pions.

- Mean field potentials are neglected, so propagation is along straight lines between elementary collisions.

- For very low particle densities the picture then reduces to independent two body collisions of hadrons in free space; data on these elementary collisions are the model inputs.

Hadron-hadron collisions have been studied in detail at AGS energies [10] [11]. The CERN-HERA compilation contains extensive listings of total and partial cross-sections over a broad range of energies [12]. Some momentum distributions appear in an LBL compilation [13], which also contains cross-section data. Fig 1 shows the measured total and elastic cross-sections for pp and for $\pi^+ p$ versus kinetic energy in the center of mass, together with the ARC fits to these total cross-sections.

Average pion multiplicities can be deduced from a study of the data for exclusive production channels. In cases where no data exists, an assumption of isospin invariance generally permits one to guess. This procedure is checked by summing the reconstructed cross-sections and seeing that one obtains the total cross-section. For $pp \rightarrow (n_\pi \pi) + X$ at energies relevant to the AGS, the average pion multiplicity (in inelastic collisions) is a roughly linear function of E_{cm}, varying from $\langle n_\pi \rangle \simeq 1$ at 2.0 GeV to $\langle n_\pi \rangle \simeq 4$ at 6.0 GeV. At higher energies, the dependence becomes logarithmic [14]:

$$< n_\pi >= a + b \log(E_{cm}) + c \log^2(E_{cm}).$$

The very large peak in the $\pi^+ p$ cross-sections is the $\Delta^{++}(1232)$ resonance. The width of that peak is 115 MeV, corresponding to a lifetime of 1.7 fm/c. Including the Lorentz boost factor, this resonance could travel several fm's, much longer than its mean free path, before decay into a proton and a pion. If the resonance is produced early on, it must interact with other particles before decaying. Similarly, other low mass baryon and meson resonances can be excited and must be allowed to interact with other stable particles as well as other

resonances. The particles, both 'stable' (not strongly decaying) and resonances, included in ARC are:

- Baryons: $p, n, \Lambda, \Sigma^+, \Sigma^0, \Sigma^-, \Xi^0, \Xi^-, \Omega^-$;
- Baryon Resonances: $\Delta^{++}, \Delta^+, \Delta^0, \Delta^-, N^{*+}, N^{*0}, Y^*, \cdots$;
- Anti-Baryons: $\bar{p}, \bar{n}, \bar{\Lambda}, \bar{\Sigma}^+, \bar{\Sigma}^0, \bar{\Sigma}^-, \cdots$;
- Mesons: $\pi^+, \pi^0, \pi^-, K^+, K^-, K^0, \bar{K}^0$;
- Meson Resonances: $\rho^+, \rho^0, \rho^-, K^*, [\omega], [\eta], [\phi], [J/\psi], \cdots$.

Collisions between particles are triggered when two particles approach within a distance $d = (\sigma/\pi)^{1/2}$, with σ evaluated in the center of mass frame for the collision. The probability for branching into different final states and the cross-section are taken from data as described above. Finally, one generates a momentum distribution for the outgoing particles. Consider pp scattering, for example: in the elastic case the momentum distribution is taken from experiment, while ARC uses simple, two parameter, fits to pp data to generate the final momentum for inelastic collisions. Outgoing momenta are generated using a Lorentz invariant final phase space:

$$\int \prod_{j=1}^{m} \frac{d^3\vec{p}_j}{(2\pi)^3 2E_j} W_t W_l \delta^4$$

the weight factor W_t limits the transverse momentum to 'soft' QCD production processes, while W_l enforces leading particle behaviour. One factor W_t is present for every final state particle and one factor W_l is included for each final leading particle.

$$W_t = e^{-p_t^2/\beta^2}$$

$$W_l = e^{-\alpha(1 \pm p_l/p_{max})}$$

Different sets α, β are used for pion production, strangeness production and antibaryon production. These parameters are fitted to pp and πp data. For instance, the ARC fit to

strangeness production in pp is reproduced in Fig 2. The data are from Blobel *et al.* [10]. The same α and β are used at all energies.

We emphasize that the ARC model is constructed using no free parameters. We have discussed parameters included in the code, but these are fixed from two body data and are *not* re-adjusted to fit $p + A$ or $A + A$ data. The philosophy followed has been to perform a careful calculation of the background from free space hadron-hadron scattering, using as little theoretical input as possible.

RESULTS

Figures 3-6 show the ARC results (solid lines) together with the experimental data points and their statistical uncertainties. We plotted the results as invariant cross sections versus transverse kinetic energy to follow the same format as the data for comparison. Detailed plots of momentum components for Cu target are given in figures 7 and 8.

The uncertainty in the simulation results isn't shown on these plots. Plots of ARC results for pions have an increasing uncertainty for high $T_\perp$ that is about 20% by $T_\perp = 1GeV$ and over 50% at the end of the curves. Because of practical limitations on computer resources, the simulation runs were done for 100000 inelastic pA events for each target. It is possible to improve the statistics at the ends by increasing the number of events. However, the kinematical region of interest for possible application in a muon collider front end is limited to low $T_\perp$. A $p_\perp$ of $500MeV/c$ corresponds to $T_\perp = 380MeV$ and the statistical uncertainty in the invariant cross sections from ARC for $T_\perp < 400MeV$ is less than 4% in all cases.

Note that the data is limited mostly to $p_\perp > 200$ MeV/c [15] whereas ARC predicts that production peaks at < 150 MeV/c, so most of the pions to be collected are expected to come from the low energy part of the spectrum where we don't have data. However, ARC fits the higher energy part of the pion spectrum, and the agreement with the proton spectra is on the 10-20% level over most of the data range. Since energy-momentum conservation is a strong constraint on the spectra this suggests that any disagreement at low momenta

should be reasonably small. Nevertheless, the absorption mechanism for low momentum pions might not be adequately modelled in ARC, and a conservative estimate is that the number of these pions could be over or under-predicted by as much as a factor of 2. It would be very useful therefore to have data in this region.

An additional uncertainty is about the angular distribution of pions at low momentum. Here, ARC seems to produce an almost isotropic distribution. This can be seen in figure 9 which depicts the pions in momentum space near the origin.

Figure 10 shows the rapidity distributions for different targets. Note that the peak is more pronounced and at lower y for heavier targets. The $p_\perp$ distributions, on the other hand, are very similar for all targets.

CONCLUSIONS

Table I lists the number of pions per interacting proton from ARC results, together with the number that have $60 < p_\perp < 360$ MeV/c, assuming those can be collected with a solenoid. In a realistic target and pion capture simulation, there are various factors that have to be taken into account which will affect the pion yield. The results we have shown assume a very thin target. Ionization energy loss, multiple Coulomb scattering, absorption, secondary production and decay in a thick target need to be considered but were not included since our initial aim was to test ARC against pA data in this note. To that end, the results show that ARC can accurately reproduce the measured pion spectrum in the range of interest. The large numbers of low momentum pions observed in simulation results is particularly interesting and it's important to know whether these could be captured efficiently to increase muon yields. The basic physics producing the peak at low momentum is not hard to understand and is surely correctly handled in ARC. The basic production in pp is biased toward lower $p_\perp$, secondary collisions take place at still lower energies, and rescattering in the nucleus further slows the pions. However the theory is not yet tested at the lower momenta where absorption of pions may become more or less significant. In

general one expects that ARC gives a pessimistic estimate of the overall pion production since it includes production channels only up to 7 pions in the final state. For these reasons, we expect the maximum pion production to occur at low momentum, but we cannot be certain about the precise numbers. Since there is no data to confirm the low end of the calculated pion spectrum, it is important that measurements be performed to settle these issues.

ACKNOWLEDGEMENTS

Y. Torun would like to thank Rick Fernow, Juan Gallardo and Harold Kirk for useful discussions. Special thanks to H. Kirk for his help with computer setup for ARC runs.

---

[1] C. L. Wang, Empirical formula for pion production in proton-proton collisions up to 1500 GeV, Phys. Rev. **D7**,2609(1973).

[2] R. B. Palmer et. al., Monte Carlo simulations of muon production, BNL Report#-61581.

[3] R. Fernow, Comparison of the Wang formula for π production with measurements at low momenta, $\mu^+\mu^-$ Collider-TN-04-94.

[4] R. Fernow, Comparison of the Wang and Wachsmut models for π production with measurements of Blobel et. al. at 12 GeV/c, $\mu^+\mu^-$ Collider-TN-03-95.

[5] R. Hagedorn and J. Ranft, Nuov. Cim. **6**,169(1968).

[6] S. H. Kahana, Yang Pang and T. J. Schlagel, In *Proceedings of Heavy Ion Physics at the AGS - HIPAGS '93*, edited by G. S. F. Stephans, S. G. Steadman and W. L. Kehoe, (13-15 Janurary, 1993), p. 263

[7] T. Abbott *et. al.*, Measurement of particle production in proton-induced reactions at 14.6 GeV/c, Phys. Rev. **D45**,3906(1992).

TABLE I. Total pion numbers

	Pions per interacting proton					
	π^+			π^-		
Target	Forward	Total	Yield	Forward	Total	Yield
Be	1.19	1.32	0.76	0.99	1.10	0.61
Al	1.47	1.69	0.91	1.27	1.46	0.79
Cu	1.60	1.90	1.02	1.47	1.76	0.93
Au	1.85	2.33	1.22	2.14	2.80	1.43

[8] T. Abbott *et. al.*, A single arm spectrometer detector system for high-energy heavy-ion experiments, Nucl. Instrum. Methods **A290**,41(1990).

[9] Y. Pang, T. J. Schlagel and S. H. Kahana, *Nucl. Phys.* **A544**, 435c (1992)
Y. Pang, T. J. Schlagel and S. H. Kahana, *Phys. Rev. Lett.* **68**, 2743 (1992)
T. J. Schlagel, Y. Pang and S. H. Kahana, *Phys. Rev. Lett.* **69**, 3290 (1992)

[10] V. Blobel, *et al. Nucl. Phys.* **B69**, 454 (1974)

[11] A. M. Rossi, *et al. Nucl. Phys.* **B84**, 269 (1975)

[12] A. Baldini, V. Flaminio, W. G. Moorhead and D. R. O. Morrison, *Total Cross-Sections for Reactions of High Energy Particles*, Landolt-Börnstein New Series, Volume **12**A and Volume **12**B, Ed. O. Madelung, (Springer Verlag, Berlin, 1988)

[13] M. E. Law, J. Kasman, R. S. Panvini, W. H. Sims, and T. Ludlam, LBL Report, No. LBL-80, (1972)

[14] L. Montanet *et. al.*, Phys. Rev. **D50**, 1173 (1994)

[15] Note that there are a couple of data points below 200 MeV/c, one with $p_\perp = 130$ MeV/c and one with $p_\perp = 180$ MeV/c but these are in high rapidity bins at $y = 2.3$ and $y = 2.5$ while most of the pions are at lower rapidities especially in targets other than Be.

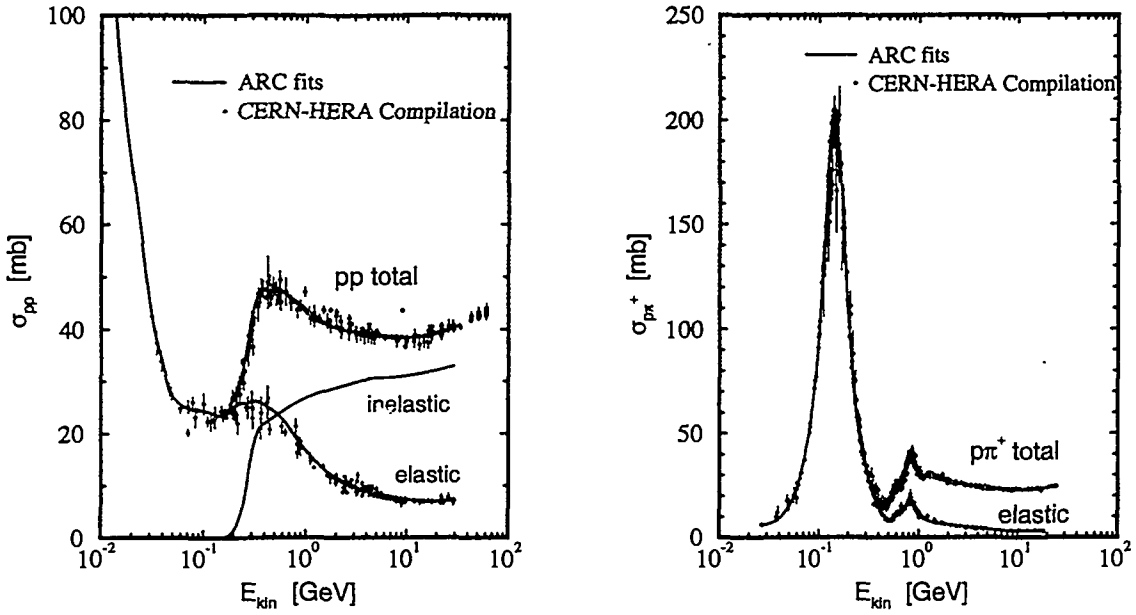

(a) (b)

FIG. 1. Two examples of measured cross-sections from the CERN-HERA compilation, shown together with the fits used in ARC: (a) the total and elastic cross-sections for pp and (b) for π^+p.

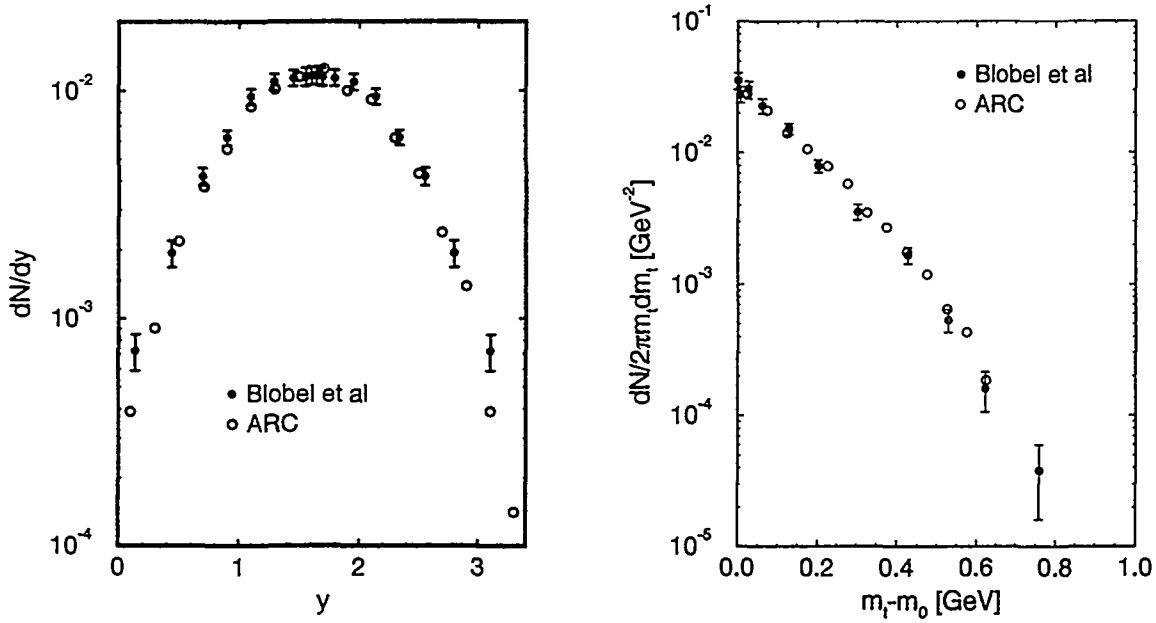

(a) (b)

FIG. 2. The K_s momentum distribution in $pp \rightarrow K_s X$ at 12 GeV/c. In ARC the absolute normalization comes from the fit to the integrated strangeness production cross-section, and the momentum distribution are selected, using Monte-Carlo, from phase space with weights W_t and W_l. The two parameters α and β which produce these distributions are part of the ARC inputs.

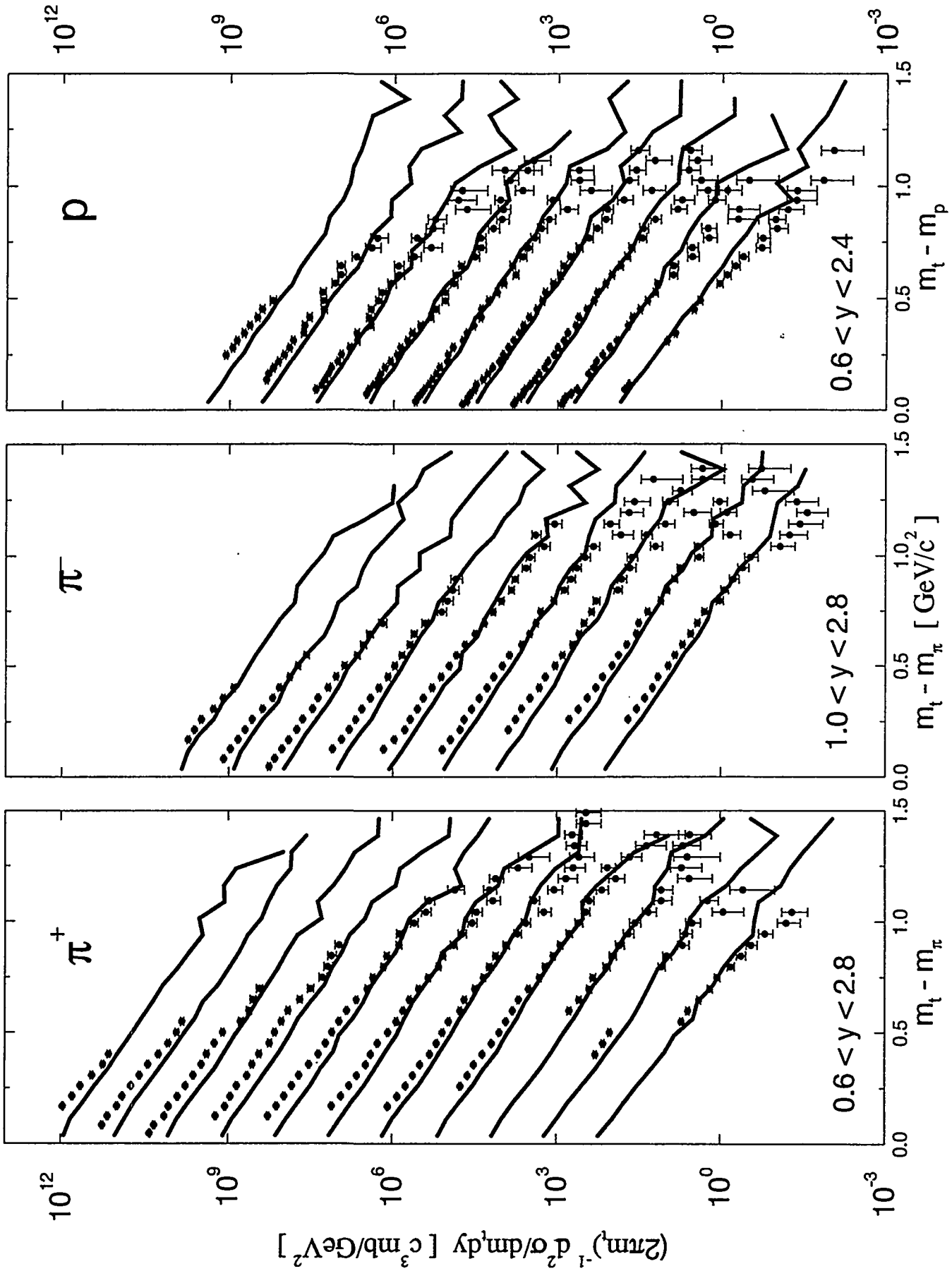

FIG. 3. Invariant cross sections for Be target. y increases from bottom to top. Successive y bins were scaled by factors of 10. Bin width is 0.2.

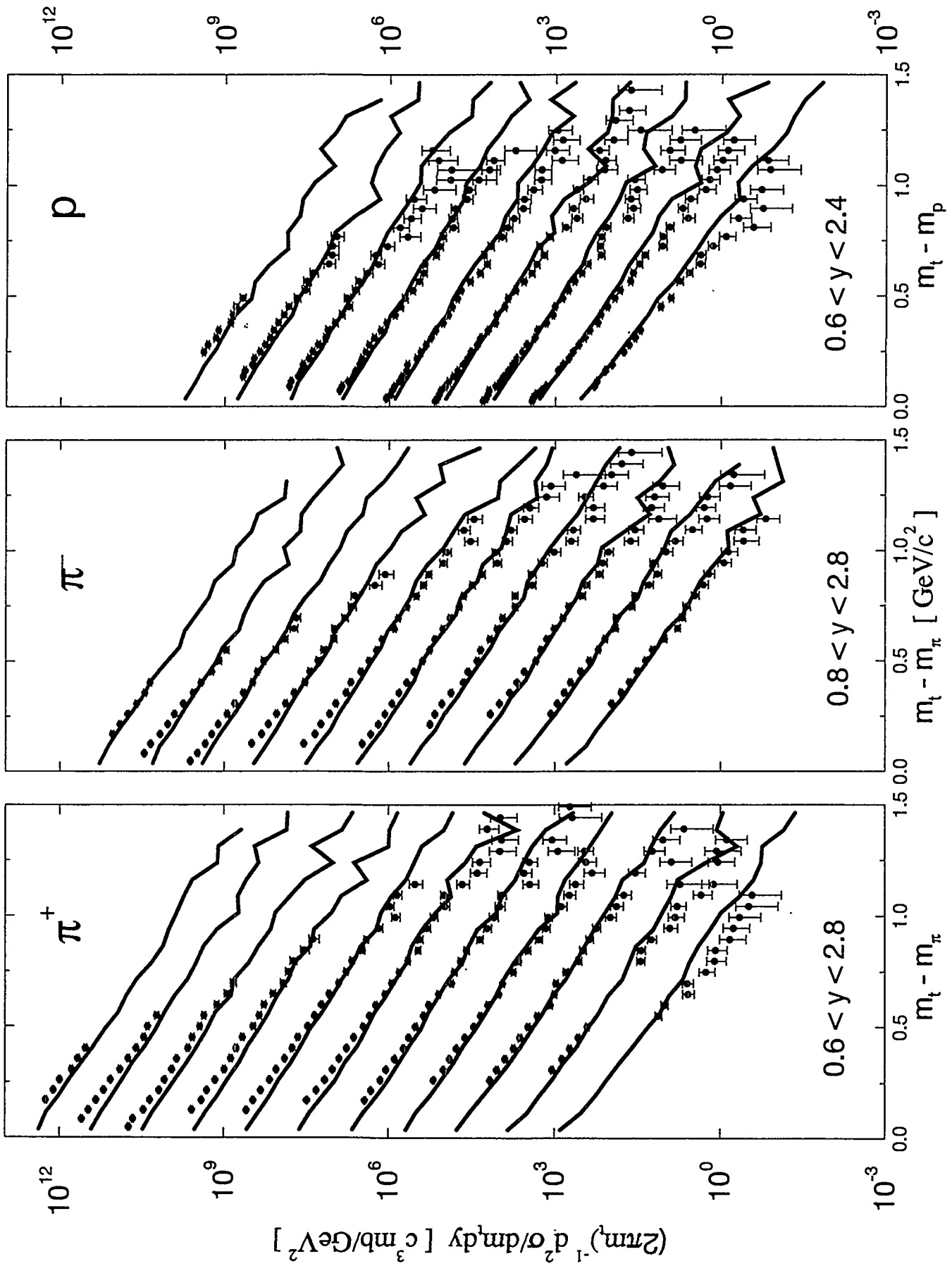

FIG. 4. Invariant cross sections for Al target

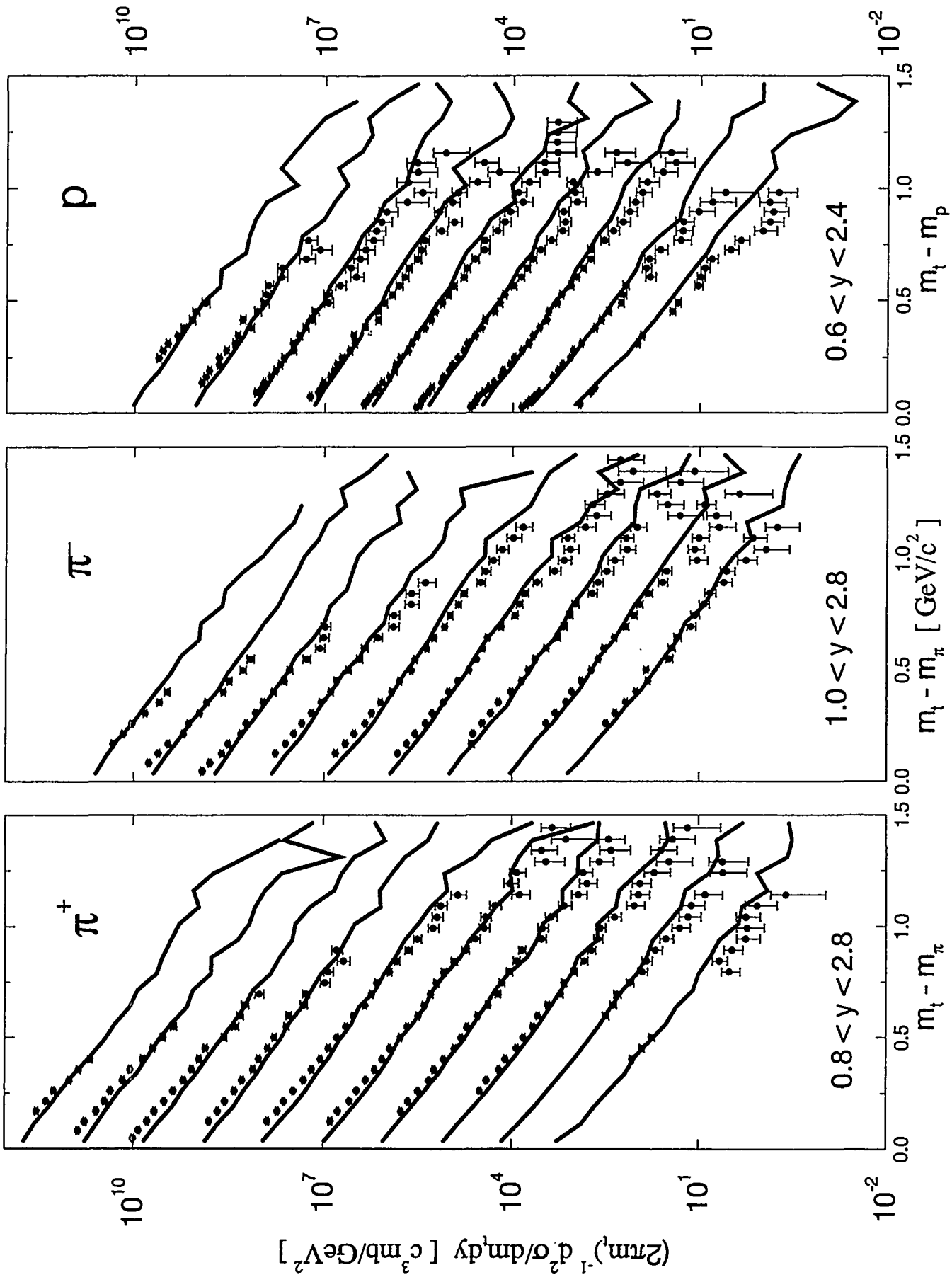

FIG. 5. Invariant cross sections for Cu target

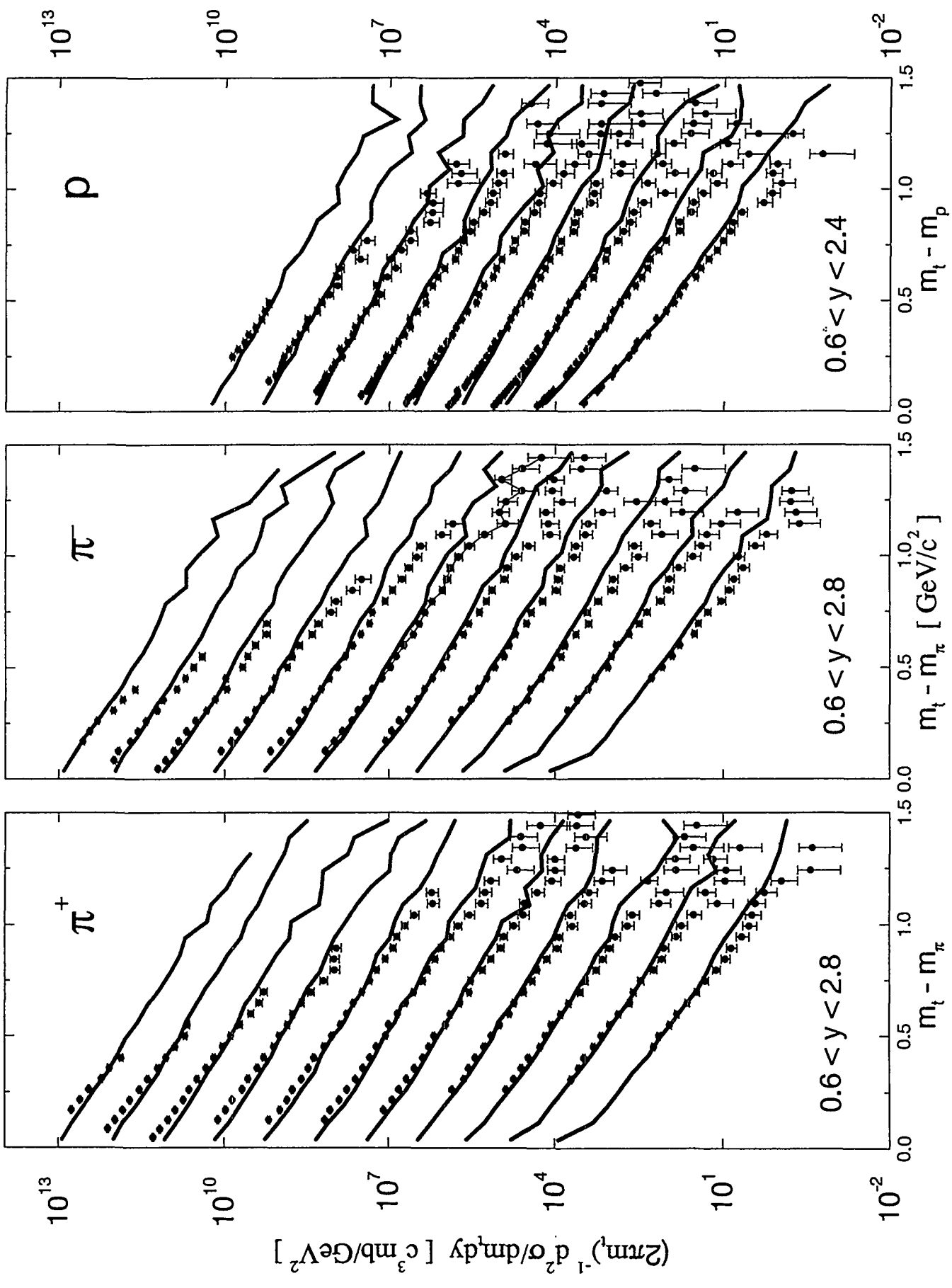

FIG. 6. Invariant cross sections for Au target

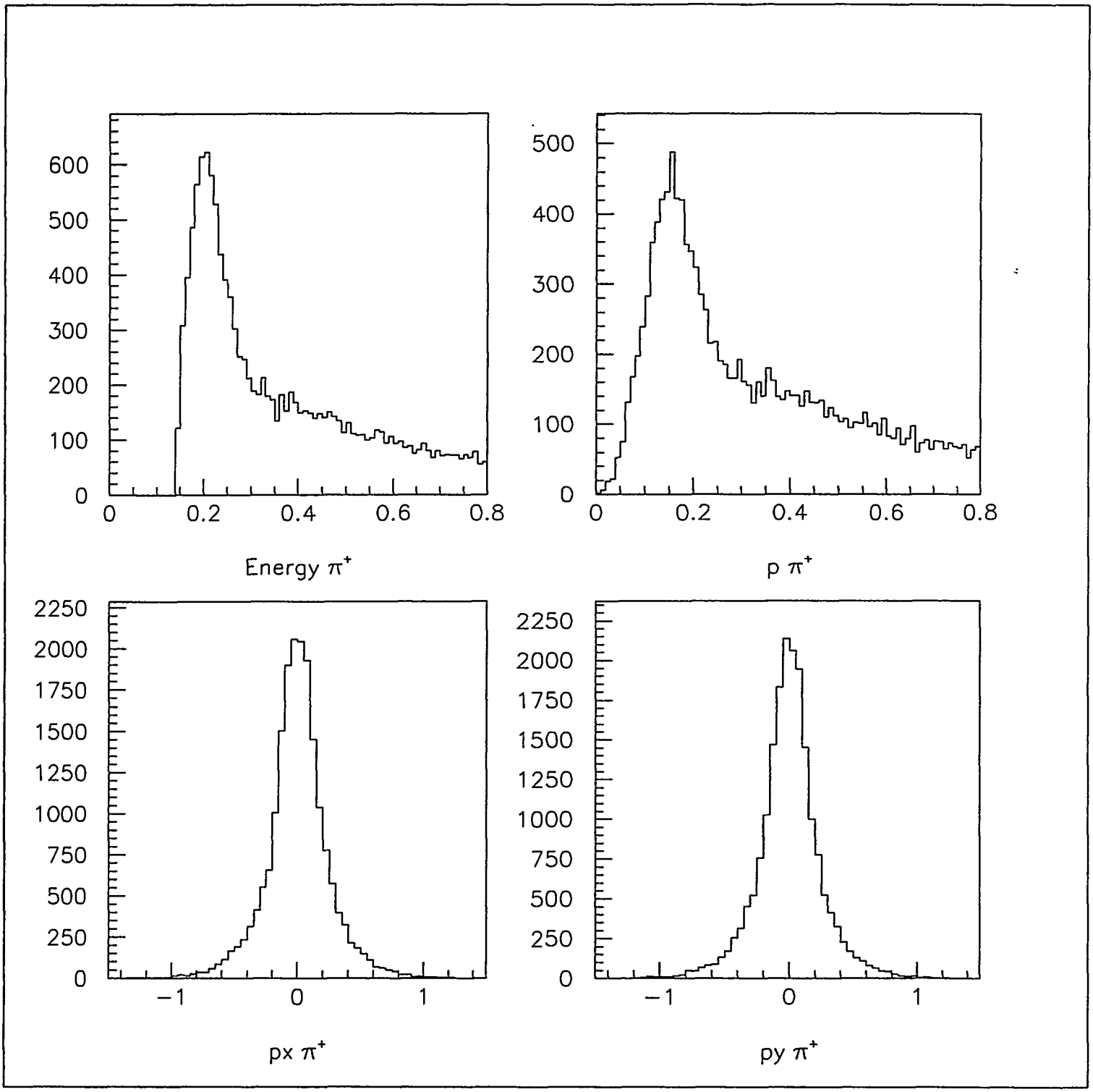

FIG. 7. Momentum components for π^+ from Cu. π^- plots are almost identical. 10000 events pictured.

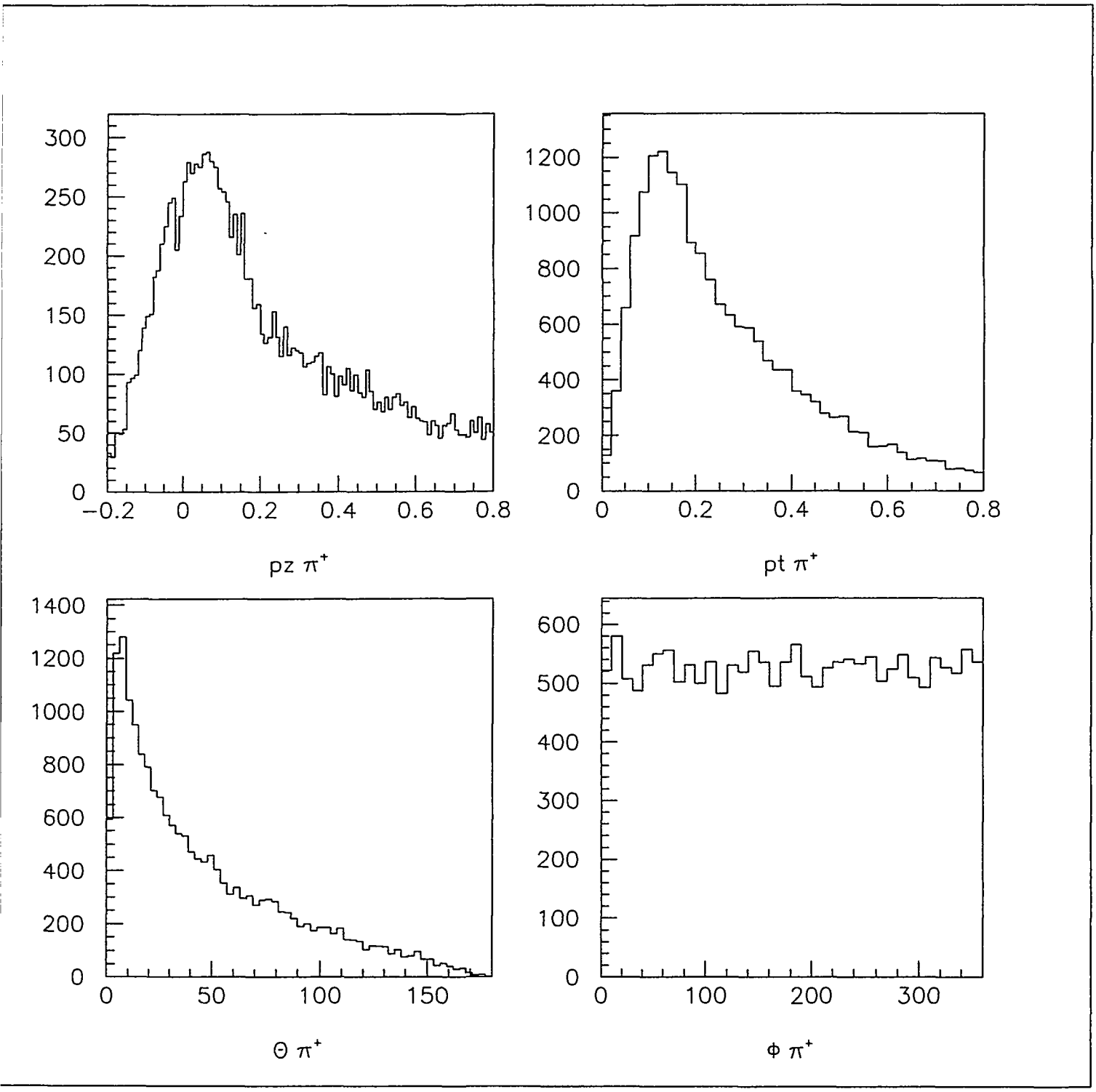

FIG. 8. Momentum components for π^+ from Cu.

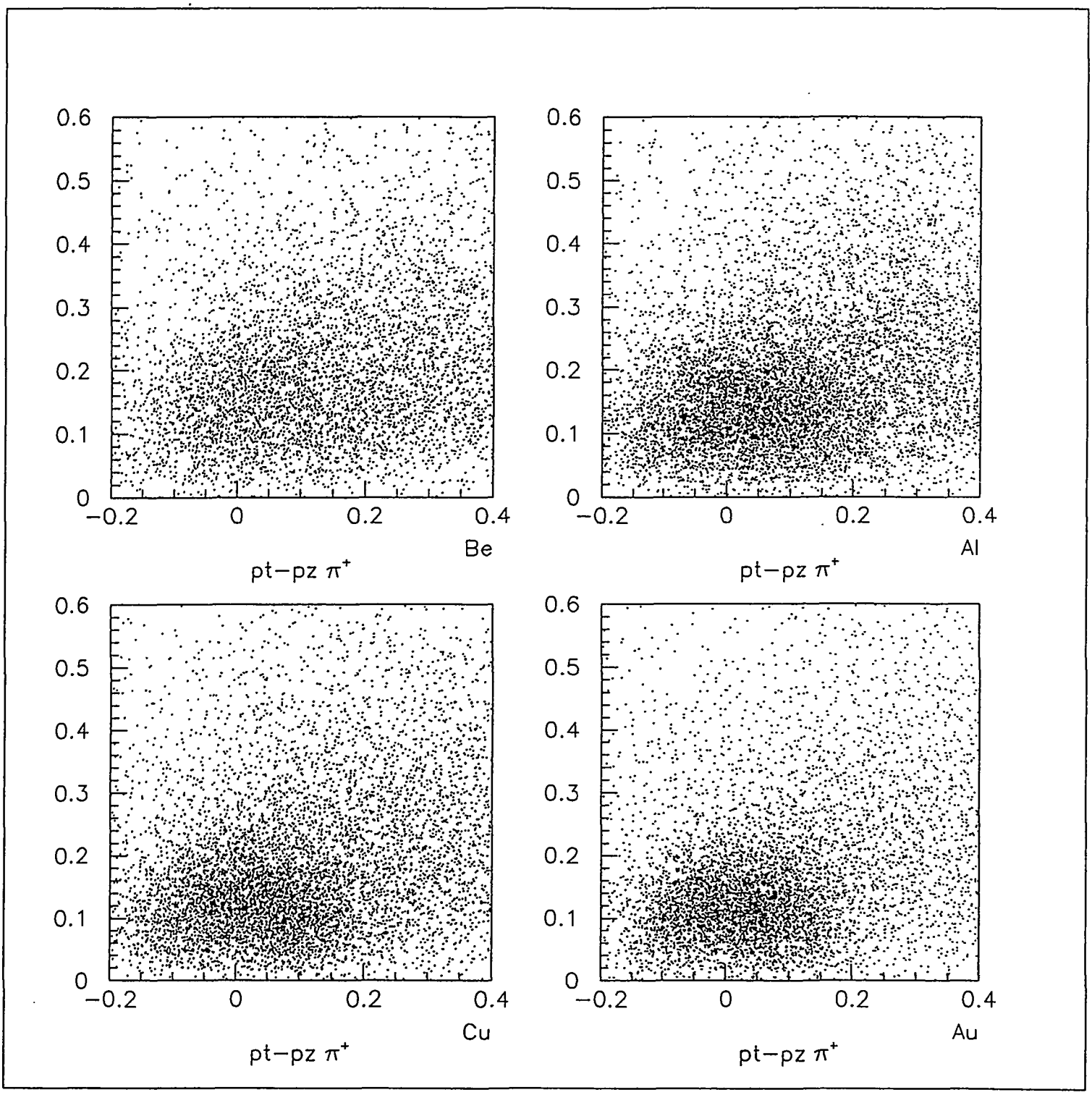

FIG. 9. Momentum space picture of pion production in ARC

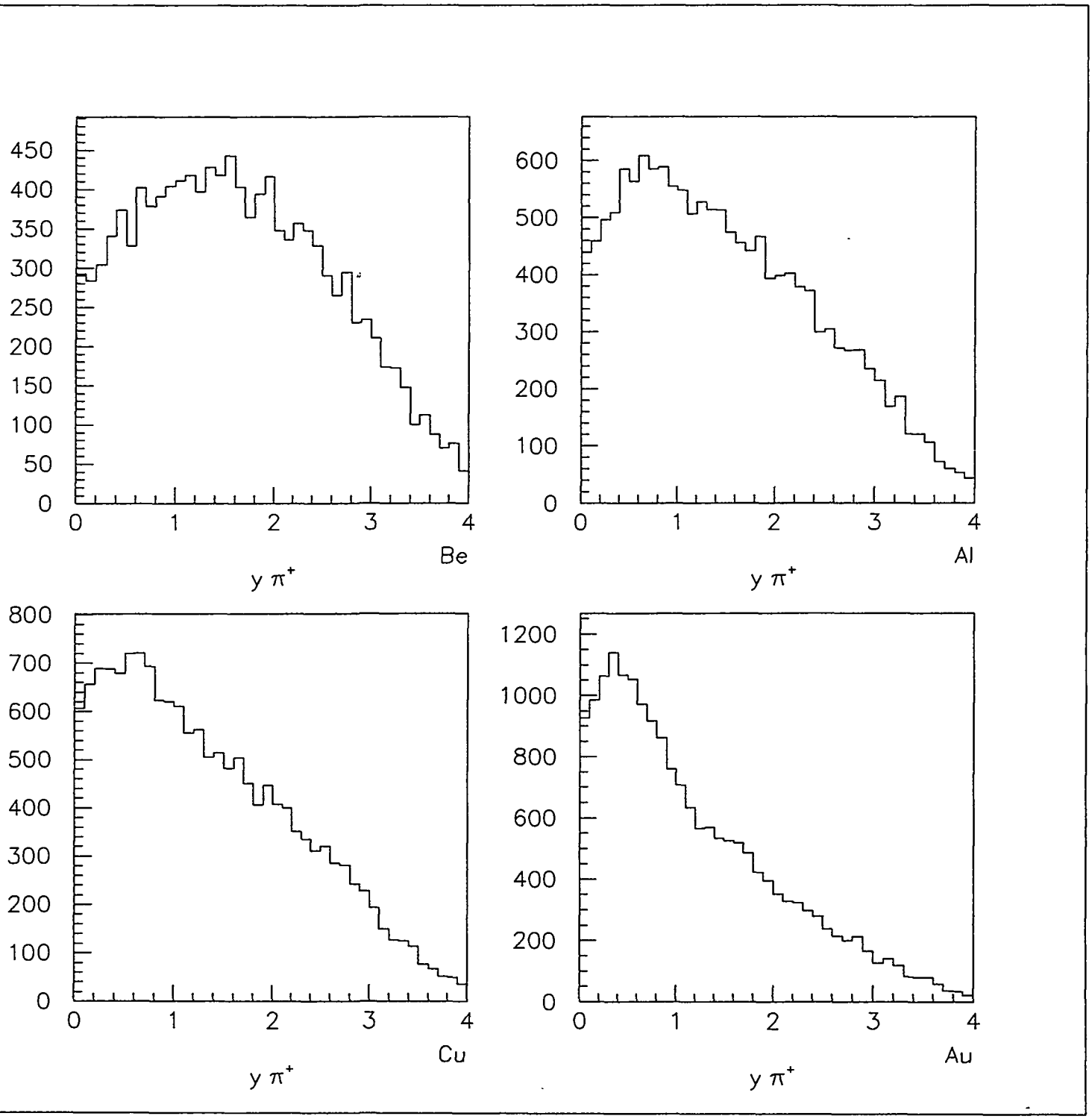

FIG. 10. Rapidity distributions from ARC